



**HAL**  
open science

**CLOUD MICROPHYSICAL PROPERTIES OF  
SUMMERTIME ARCTIC STRATOCUMULUS  
DURING THE ALOUD CAMPAIGN:  
COMPARISON WITH PREVIOUS RESULTS IN THE  
EUROPEAN ARCTIC**

Régis Dupuy, Olivier Jourdan, Guillaume Mioche, A Ehrlich, F Waitz,  
Christophe Gourbeyre, E Järvinen, M. Schnaiter, Alfons Schwarzenboeck

► **To cite this version:**

Régis Dupuy, Olivier Jourdan, Guillaume Mioche, A Ehrlich, F Waitz, et al.. CLOUD MICROPHYSICAL PROPERTIES OF SUMMERTIME ARCTIC STRATOCUMULUS DURING THE ALOUD CAMPAIGN: COMPARISON WITH PREVIOUS RESULTS IN THE EUROPEAN ARCTIC. 15th Conference on Cloud Physics, 2018, Vancouver, Canada. hal-01932907

**HAL Id: hal-01932907**

**<https://hal.science/hal-01932907v1>**

Submitted on 23 Nov 2018

**HAL** is a multi-disciplinary open access archive for the deposit and dissemination of scientific research documents, whether they are published or not. The documents may come from teaching and research institutions in France or abroad, or from public or private research centers.

L'archive ouverte pluridisciplinaire **HAL**, est destinée au dépôt et à la diffusion de documents scientifiques de niveau recherche, publiés ou non, émanant des établissements d'enseignement et de recherche français ou étrangers, des laboratoires publics ou privés.

# 71 CLOUD MICROPHYSICAL PROPERTIES OF SUMMERTIME ARCTIC STRATOCUMULUS DURING THE ACLOUD CAMPAIGN : COMPARISON WITH PREVIOUS RESULTS IN THE EUROPEAN ARCTIC

Regis Dupuy<sup>\*1</sup>, O. Jourdan<sup>1</sup>, G. Mioche<sup>1</sup>, A. Ehrlich<sup>2</sup>, F. Waitz<sup>3</sup>, C. Gourbeyre<sup>1</sup>, E. Järvinen<sup>3</sup>, M. Schnaiter<sup>3</sup>, and A. Schwarzenboeck<sup>1</sup>

(1) Laboratoire de Météorologie Physique CNRS/UCA UMR 6016, Aubière, France; (2) University of Leipzig, Leipzig, Germany; (3) Karlsruhe Institute of Technology, Karlsruhe, Germany

## 1. INTRODUCTION

The Arctic region is more sensitive to climate change than any other region of the Earth (Solomon, 2007). Clouds and particularly low-level cloud related processes have a major impact on the Arctic surface energy budget (Curry, 1995; Curry, 1996; Morrison, 2011). Observations suggest that boundary layer mixed phase clouds (MPC, mixture of liquid droplets and ice) are ubiquitous in the Arctic and persist for several days under a variety of meteorological conditions (Mioche, 2015; Morrison, 2012; Shupe, 2011; Shupe and Intrieri, 2004). They occur as single or multiple stratiform layers of supercooled droplets near the cloud top from which ice crystals form and precipitate (Mioche, 2017). The microphysical properties of these clouds have a large impact on the surface radiative fluxes and Arctic climate feedbacks (Kay, 2012; Kay and Gettelman, 2009) but are often poorly predicted by models (Forbes and Ahlgrimm 2014). In particular, a correct representation of MPC ice nucleation process and liquid-ice partitioning in numerical models is needed for both weather forecasts and climate prediction (Barret, 2017a,b).

In May-June 2017, a suite of "in situ" microphysical probes was deployed on-board the AWI Polar 6 aircraft during the ACLOUD experiment in the Svalbard region (Arctic Cloud Observations Using airborne measurements during polar Day). ACLOUD is a joint project of different German universities and research institutes embedded in the Transregional collaborative research center (AC)3. The general goal of ACLOUD is to gather a comprehensive data set of what will contribute to a process level understanding of clouds in the Arctic and their role in the amplified climate change observed in this region.

This campaign gave us the opportunity to explore the microphysical properties of summer arctic stratocumulus clouds over different surface conditions (open sea, sea ice and marginal sea ice zone). Cloud vertical profiles of liquid and ice water content, number concentration and effective size are presented under different surface conditions air mass origin.

These results are compared to previous studies from Lloyd (2015) performed during the ACCACIA campaign (summer/spring cloud over open sea), Young (2016), spring cloud transition from sea ice to open sea) as well as with cloud vertical profiles

established by Mioche et al. (2017) over the Greenland and Barents seas. Hereafter, these studies will be referred as L15, Y16 and M17 respectively.

## 2. INSTRUMENTATION

The instrumentation used in the present study was installed on the Polar 6 aircraft of the Alfred Wegener Institute (AWI). It is a modified DC-3 aircraft of the type Basler BT-67 with an endurance of up to 2300 km and a ceiling of 7.6 km altitude. Its cruise speed is between 10 and 150 knots and can operate for 6 to 7 hours with a take-off weight of 14 tons.

The Small Ice Detector (SID-3) instrument (Kaye, 2008; Vochezer, 2016) measures the size distribution of cloud particles from 5 to 50  $\mu\text{m}$ . From a sub-sample of particles the spatial intensity distribution of the light scattered in the angular range of  $7^\circ$  to  $23^\circ$  is recorded as a two-dimensional scattering pattern. These patterns can be analyzed for the particle shape and sub-micrometer scale complexity (Vochezer, 2016; Schnaiter, 2018).

The Cloud Droplet Probe (CDP) is a forward scattering optical spectrometer using a single mode diode laser at a wavelength of 0.658  $\mu\text{m}$  (Lance, 2010; Wendisch, 1996). The instrument counts and sizes individual droplets by detecting pulses of light scattered from a laser beam in the near-forward direction ( $4^\circ - 12^\circ$ ), (using a calibrated sample area of 0.32  $\text{mm}^2$ ). Sizes are accumulated in 30 bins with variable sizes (1  $\mu\text{m}$  wide for size lower than 14  $\mu\text{m}$  or 2  $\mu\text{m}$  wide for larger droplets). The CDP was equipped with anti-shattering tips to reduce possible shattering artifacts (Korolev, 2011). Microphysical quantities were derived from the measurements, such as liquid water content (LWC) and effective droplet diameter ( $D_{\text{eff}}$ ) by integrating the cloud particle number size distribution (PNSD). The acquired PNSDs have been corrected to minimize the effect of Mie sizing ambiguities using a Monte Carlo inversion method.

The Cloud Imaging Probe (CIP) and the Precipitation Imaging Probe (PIP) measure the size and shape of cloud and precipitation particles (Baumgardner, 2011). The measurement principle of these Optical Array Probes (OAPs) is based on the linear array technique to acquire the two-dimensional black and white images of particles. As the particles pass through a laser beam, the shadow they cast on a photodiode array is used to record their dimensions. The PNSDs are computed from the OAP images, but the assessment of the median mass diameter (MMD) and the ice water content (IWC) relies on the definition of the crystal diameter and its mass-

---

\* Corresponding author address : Regis Dupuy, LaMP, Bat. Physique 8, 4 Avenue Blaise Pascal, TSA 60026, CS 60026, 63178 AUBIERE CEDEX, FRANCE

diameter relationship (Brown and Francis 1995). Possible contamination of shattering/splashing of ice/liquid particles on the instruments tips have been identified and removed using inter arrival time statistics (Field, 2006) and image processing.

A similar instrument payload was used for L15, Y16 and M17 dataset and a comparison of every instrumentations can be seen in table 1.

Cloud Probes	Size Range	Parameters
Polar Nephelometer (PN)	Few $\mu\text{m}$ to $\sim 800 \mu\text{m}$	Scattering phase function, asymmetry parameter (g), extinction coef.
Forward Scattering Probe (FSSP)	3 $\mu\text{m}$ to 45 $\mu\text{m}$	Droplets size distribution, LWC
Cloud Particle Imager (CPI)	$\sim 15 \mu\text{m}$ to 2.3 mm	Ice particle size distribution, shape, IWC
2D-Stereo (2D-S)	$\sim 10 \mu\text{m}$ to 1.3 mm	Ice particle size distribution, shape, IWC
Cloud Droplet Probe (CDP)	3 $\mu\text{m}$ to 45 $\mu\text{m}$	Droplets size distribution, LWC
Cloud Droplet Probe (CDP)	3 $\mu\text{m}$ to 45 $\mu\text{m}$	Droplets size distribution, LWC
Small Ice Detector (SID3)	3 $\mu\text{m}$ to 45 $\mu\text{m}$	Droplets size distribution, LWC
Cloud Image Probe (CIP)	$\sim 25 \mu\text{m}$ to 1.6 mm	Ice particle size distribution, shape, IWC

Table1 : List of the probes used for M17 study (in red), ACCACIA campaign (L15 and Y16 studies, in blue) and this study (in black) to characterize the liquid and ice properties of the Arctic Stratocumulus Clouds.

### 3. DATA PROCESSING AND CLUSTERING

#### 3.1. Meteorological conditions

The meteorological conditions used in this study are precisely described in M17 and Knudsen (2018). Table 2 summarizes the synoptic regimes encountered during the airborne campaigns. Mean cloud top temperature (CTT) and air mass origin (based on HYSPLIT back trajectory computation) are also displayed as they are used in our cloud observation classification.

Since the temperature was always above  $-15^\circ\text{C}$  during ACLOUD, the M17 COLD regime was not included in the comparison.

#### 3.2. Liquid / Ice discrimination

The discrimination of liquid and ice particle samples is based on the circularity of particles (see Crosier et al., 2011). Cloud particle images with value larger than 1.25 are classified as ice crystals. This method is only valid for images of particles with surface larger than 16 pixels and induces that the

minimum diameter of particles identified as ice crystal is 125 microns for the CIP. In order to be consistent with previous studies, only particles with size lower than  $50 \mu\text{m}$  are considered to be liquid water droplets.

Regime	CTT	Air Mass origin	# Flights (# vertical profiles)
M17 COLD	< $-15^\circ\text{C}$	North (Central Arctic) or Greenland	6
M17 WARM North	> $-15^\circ\text{C}$	North (Central Arctic) or Greenland	7
M17 WARM South	> $-15^\circ\text{C}$	South (Europe)	5
ACLOUD Cold	> $-15^\circ\text{C}$	North (Central Arctic)	1 (4)
ACLOUD Normal	> $-15^\circ\text{C}$	North (Central Arctic)	5 (25)
ACLOUD Warm	> $-15^\circ\text{C}$	South (Europe) or Greenland	4 (37)

Table2 : List of meteorological periods and their associated number of flights defined by M17 (in red) and Knudsen (2018). The number of vertical profiles has been added in brackets for ACLOUD.

#### 3.3. Surfaces overflow

The classification of the underlying surface is based on the average sea ice concentration measurements produced by the University of Bremen from AMSR2 satellite data) :

- Above 90 % is defined as “Sea Ice” (SI)
- Between 10 and 90 % is the “Marginal Ice Zone” (MIZ)
- Lower than 10% is defined as “Open Water” (OW)
- Land correspond to NaN values.

It is important to note that **M17 cloud samples were only taken over open water.**

#### 3.4. Altitude normalization

Since cloud top and cloud base heights exhibit large variability, the altitudes are normalized following the method presented in M17. The cloud top and cloud base refer to the liquid phase layer, i.e., the cloud layers containing liquid droplets (mixed-phase or liquid only). The liquid layer is identified based on the CDP and the CIP measurements. when the liquid water content is greater than  $0.001 \text{ g/m}^3$ , the liquid extinction is above  $1 \text{ km}^{-1}$  and the ice extinction is lower than  $0.5 \text{ km}^{-1}$ .

Within the liquid layers (Eq. 1) and below the cloud base (Eq. 2) the normalized altitudes  $Z_n$  are defined as follows :

$$Z_n = \frac{Z - Z_b}{Z_t - Z_b} \quad \text{for } z_b < z < z_t \quad (1)$$

$$Z_n = \frac{Z}{Z_b} - 1 \quad \text{for } z < z_b, \quad (2)$$

where  $Z_n$  is the normalized altitude,  $Z$  the altitude corresponding to the aircraft measurements, and  $Z_t$  and  $Z_b$  the cloud top and base altitudes, respectively. Thus,  $Z_n = 1$  corresponds to the top-of-the-cloud liquid-containing layer and 0 to its base. Negative values characterize regions of ice precipitation below the cloud layer and the altitude of  $-1$  defines the ground level according to Eq. (2).

To obtain representative statistical results, the cloud layers have been stratified in 10 levels with intervals of  $Z_n = 0.2$ . The vertical profiles of MPC microphysical properties presented hereafter are obtained by averaging the *in situ* measurements over each normalized altitude layer.

## 4. RESULTS

### 4.1. Dataset statistical robustness

To characterize the robustness of our statistical analyses, Table 3 and 4 show the number of samples within each data cluster according to the underlying surface and the meteorological conditions. Each sample represent a 10 second average of the measurements performed by ALOUD probes (lowest time resolution of the SID3).

These tables show that nearly no sampling was performed over Land. Thus the "over land" measurements sub-sample will not be included in the following.

LIQUID samples	Cold Period	Normal Period	Warm Period
Sea Ice > 90%	0	1019	1146
90% > MIZ > 10%	307	48	556
10% > Open Water	56	419	548
Land	0	45	0

Table 3 : Number of 10 second averaged samples of the cloud liquid phase for each cluster defined by the meteorological conditions and surfaces overflow during ALOUD campaign.

ICE samples	Cold Period	Normal Period	Warm Period
Sea Ice > 90%	0	297	1357
90% > MIZ > 10%	93	9	676
10% > Open Water	21	264	49
Land	0	26	0

Table 4 : Number of 10 second averaged samples of the cloud ice phase for each cluster defined by the meteorological conditions and surfaces overflow during ALOUD campaign.

The cold period is hardly representative as well as the MIZ during the normal period. However since cold and normal periods exhibit similar air mass origins and mean cloud top temperature, these two periods are merged leading to the following clusters :

- ALOUD North = Cold Period + Normal Period
- ALOUD South = Warm Period

The cloud vertical profiles are computed separately for each of these dataset clusters and presented in the following section for a better analysis and discussions of the results.

## 4.2. Vertical Profiles

### a) Summer / Spring comparison

Figure 1 shows the cloud vertical profiles for the liquid phase over open water in Spring and in Summer. Higher liquid water content is found in Summer (ALOUD) compared to M17 Warm North. However similar values and behavior are encountered when comparing the summer profiles to the Spring M17 Warm South LWC data. Significant discrepancies in the droplet number concentrations are observed. High droplet concentrations are associated with low effective sizes and air mass originating from the South. This could be indicative of a possible Twomey effect but aerosol concentration are still needed to confirm these first results.

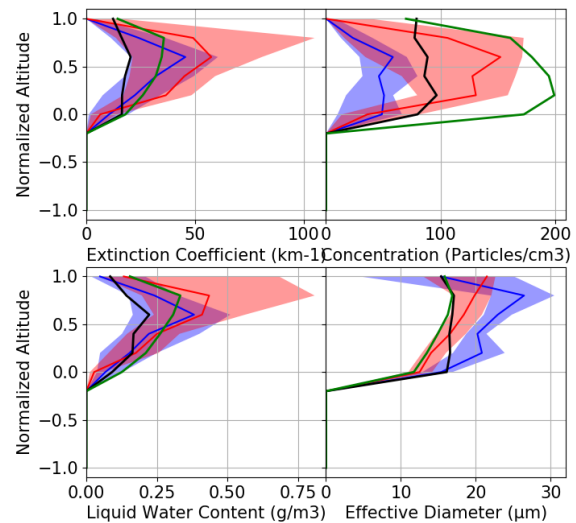


Figure 1 : Vertical profiles (normalized altitudes) of liquid droplet extinction coefficient (a), number concentration (b), mass content (c) and effective diameter (d) median values for ALOUD North (blue line), ALOUD South (red line), M17 Warm North (black line) and M17 Warm South (green line). Shade of blue and red represent the interquartile values for ALOUD North and ALOUD South respectively.

While an earlier study by Lloyd (2015) has shown that five times more ice crystal concentrations were found in summer than in spring in this region over open water, few ice crystals are measured over open water ( $<1L^{-1}$ ) during ALOUD (cf. Fig. 2). Ice crystals are mainly found in the lowest cloud layer but no general trend can be depicted as the ice properties show a large variability. It is important to note though

that L15 was based on only one flight and may not be statistically comparable.

Nevertheless, the ice particles properties (concentration and size) measured over the MIZ with south air mass origin seem similar to the spring cases over open water with the same air mass origin.

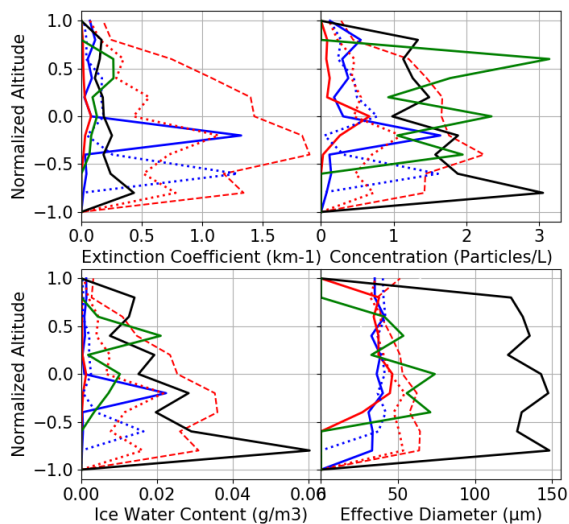


Figure 2 : vertical profiles (normalized altitudes) of large ( $D_p > 125 \mu\text{m}$ ) ice crystals extinction coefficient (a), number concentration (b), mass content (c) and effective diameter (d) median values for open water (full line), marginal ice zone (dashed lines) and sea ice (dotted lines) surfaces overflow during ACLUD North (blue lines), ACLUD South (red lines), M17 Warm North (black line) and M17 Warm South (green line) meteorological conditions.

### b) Impact of the underlying surface

Figure 3 shows that the main differences observed in the liquid phase properties can be attributed to the large scale meteorological conditions and the air mass origin (fewer and larger droplets during Normal-Cold period) linked to the aerosol concentrations.

However, changes in droplet concentration values with the underlying surface are also observed. Over MIZ and under southerly flow, a higher droplet concentration is found at cloud top followed by a steep decrease at lower levels. This could be indicative of changes in the droplet activation conditions (supersaturation, heat flux...) linked to the surface type. Ice crystal concentrations show that  $\text{MIZ} > \text{SI} > \text{OW}$  with a maximum of  $2\text{L}^{-1}$ .

These trends have to be compared to previous results of Young (2016) who showed that:

- Ice crystal properties were constant with surfaces with concentrations between  $0.5$  and  $1.5\text{L}^{-1}$
- Droplet concentration :  $\text{MIZ} > \text{SI} > \text{OW}$

Yet, these measurements were conducted in March during one flight only and a mean top cloud temperature of  $-20^\circ\text{C}$ .

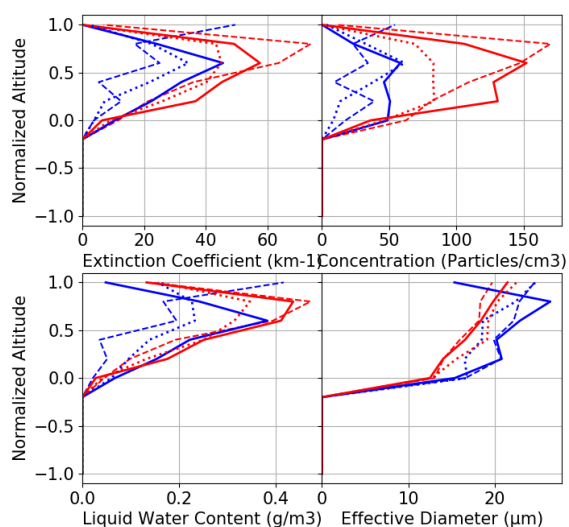


Figure 3 : vertical profiles (normalized altitudes) of liquid droplet extinction coefficient (a), number concentration (b), mass content (c) and effective diameter (d) median values for open water (full line), marginal ice zone (dashed lines) and sea ice (dotted lines) surfaces overflow during ACLUD North (blue lines) and ACLUD South (red lines) meteorological conditions.

### 4.3. Outlooks

The study presented in this poster is a preliminary study. We plan to carry on by first analyzing the aerosol concentration of particles larger than  $100 \text{ nm}$  to study their impact on cloud droplets. Particles larger than  $500 \text{ nm}$  will be considered to investigate their impact as Ice Nuclei. This study will also be combined with an other study on small ice crystals performed by F. Waitz (see poster 72). Future campaigns are planned in this region (AFLUX 2019 and MOSAIC 2020) in order to increase the number of cloud samples with different air mass origins and surfaces overflow.

### 5. ACKNOWLEDGMENT AND REFERENCES

This work was primarily funded by EECLAT project (Expecting EarthCare, Learning from A-Train) supported by the french Centre National des Etudes Spatiales (CNES). We gratefully acknowledge the support from the Transregional Collaborative Research Center (TR 172) "Arctic Amplification: Climate Relevant Atmospheric and SurfaCe Processes, and Feedback Mechanisms (AC)3", which is funded by the German Research Foundation (Deutsche Forschungsgemeinschaft; DFG) and from the Chantier Arctique - Pollution in the Arctic System (PARCS) project, funded by CNRS. The authors thank the Alfred Wegener Institute (AWI) team for managing and operating aircrafts in the arctic.

Brown, P. R. A. and Francis, P. N., 1995 : Improved Measurements of the Ice Water Content in Cirrus Using a Total-Water Probe, *J. Atmos. Ocean. Tech.*, 12, 410–414.

Crosier, J. and al., 2011 : Observations of ice multiplication in a weakly convective cell embedded in

supercooled mid-level stratus, *Atmos. Chem. Phys.*, 11, 257-273,  
Mioche, G., and al., 2017 : Characterization of Arctic mixed-phase cloud properties at small scale and coupling with satellite remote sensing, *Atm. Chem. Phys.*, 17, 12845–12869,  
Knudsen, E. M. and al., 2018 : Synoptic development during the ACLOUD/PASCAL field campaign near Svalbard in spring 2017, *Atmos. Chem. Phys. Discuss.*, in review.

Lloyd, G. and al., 2015 : Observations and comparisons of cloud microphysical properties in spring and summertime Arctic stratocumulus clouds during the ACCACIA campaign, *Atmos. Chem. Phys.*, 15, 3719-3737.  
Young, G. and al., 2016 : Observed microphysical changes in Arctic mixed-phase clouds when transitioning from sea ice to open ocean, *Atmos. Chem. Phys.*, 16, 13945-13967.